Selected tight-binding models

Andriy Zhugayevych (http://zhugayevych.me)

December 18, 2022

§1. Abbreviations and notations

a3p	Ahlrichs triple-ζ basis Def2-TZVP	NAO	Natural Atomic Orbital
AO	Atomic Orbital	NBO	Natural Bonding Orbital
CB	Conduction Band	NO	Natural Orbital
DFT	Density Functional Theory	NTO	Natural Transition Orbital
HOMO	Highest Occupied Molecular Orbital	PAW	Projector Augmented Wave
LMO	Localized Molecular Orbital	p2p	Pople double-ζ polarized basis 6-31G*
LP	Lone Pair	SCF	Self-Consistent Field
LUMO	Lowest Unoccupied Molecular Orbital	TB	Tight Binding
MO	Molecular Orbital	VB	Valence Band

The inverse mass tensor reported here should be divided by $\hbar^2/m_\mathrm{e} \approx 7.6200$ eVÅ^2 to obtain dimensionless masses.

§2. Graphene π-system

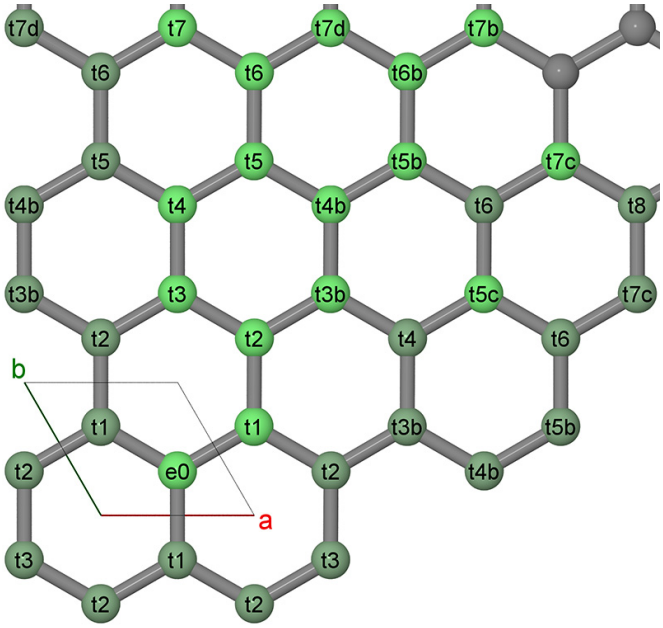

Figure 1: Symmetry unique TB elements of graphene π-system. See also Fig. 29.

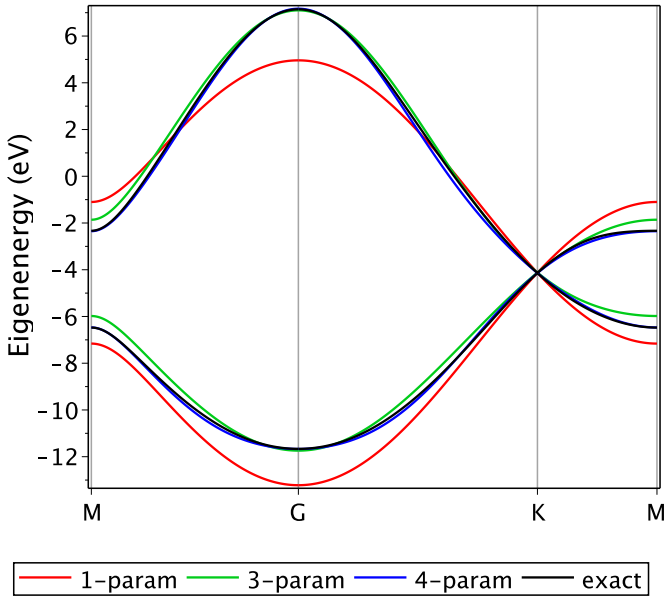

Figure 2: Energy bands of graphene π-system for a series of models of increasing accuracy.

The symmetry unique TB elements are shown in Fig. 1. Because there are 5 high-symmetry energy reference values at 3 k-points: Γ, K and M, the largest 'fittable' model includes the onsite energy ε_0 and 4 transfer integrals including 3 directly interacting pairs: t_1, t_2, t_3. The 4th integral should be t_4 to balance the accuracy of diagonal and off-diagonal Hamiltonian matrix elements containing even and odd (by chemical distance) transfer integrals respectively. The resulting Hamiltonian is given by

$$H_{11} = H_{22} = \varepsilon_0 + 2t_2\left(\cos k_1 + \cos k_2 + \cos k_3\right) + 2t_4\left(\cos(k_1 - k_2) + \cos(k_2 - k_3) + \cos(k_3 - k_1)\right),$$
$$H_{12} = t_1\left(1 + \mathrm{e}^{\mathrm{i}k_1} + \mathrm{e}^{-\mathrm{i}k_2}\right) + t_3\left(\mathrm{e}^{\mathrm{i}(k_1-k_2)} + \mathrm{e}^{\mathrm{i}k_3} + \mathrm{e}^{-\mathrm{i}k_3}\right) \tag{2.1}$$

where $k_3 = -k_1 - k_2$. Therefore $E_{1,2} = H_{11} \mp |H_{12}|$. In high-symmetry direction $k_1 = k_2 = k$:

$$H_{11} = \varepsilon_0 + 2t_2\left(2\cos k + \cos 2k\right) + 2t_4\left(1 + 2\cos 3k\right), \quad H_{12} = t_1\left(1 + 2\cos k\right) + t_3\left(1 + 2\cos 2k\right). \tag{2.2}$$

In high-symmetry direction $k_1 = k$, $k_2 = 0$:

$$H_{11} = \varepsilon_0 + 2t_2\left(1 + 2\cos k\right) + 2t_4\left(2\cos k + \cos 2k\right), \quad H_{12} = t_1\left(2 + \mathrm{e}^{\mathrm{i}k}\right) + t_3\left(2\mathrm{e}^{\mathrm{i}k} + \mathrm{e}^{-\mathrm{i}k}\right). \tag{2.3}$$

In high-symmetry points ($k = \{0, \pi, 2\pi/3\}$):

$$E(1/3, 1/3) = \varepsilon_0 - 3t_2 + 6t_4, \qquad E_{1,2}(0,0) = \varepsilon_0 + 6t_2 + 6t_4 \mp (3t_1 + 3t_3),$$
$$E_{1,2}(1/2, 0) = E_{1,2}(1/2, 1/2) = \varepsilon_0 - 2t_2 - 2t_4 \mp (t_1 - 3t_3). \tag{2.4}$$

In particular, if we fit parameters at these high-symmetry points to PBE/p2p calculations, we obtain (in eV):

$$\varepsilon_0 = -3.87,\ t_1 = -2.87,\ t_2 = 0.21,\ t_3 = -0.27,\ t_4 = 0.06,$$

giving band structure visually coinciding with the exact one. Although t_4 is small, neglecting it results in large error at M-point. The minimal model (t_1 only) is still qualitatively accurate. Exact TB integrals fade with distance quickly:

$$\varepsilon_0 = -3.778,\ t_1 = -2.887,\ t_2 = 0.218,\ t_3 = -0.239,\ t_4 = 0.046,\ t_{5c} = -0.029,\ t_{4b} = -0.015,$$
$$t_{3b} = 0.004,\ t_{5b} = 0.004,\ t_6 = 0.003,\ t_{6b} = -0.002,\ t_5 = 0.001, \ldots$$

§3. Graphene σ-valence band

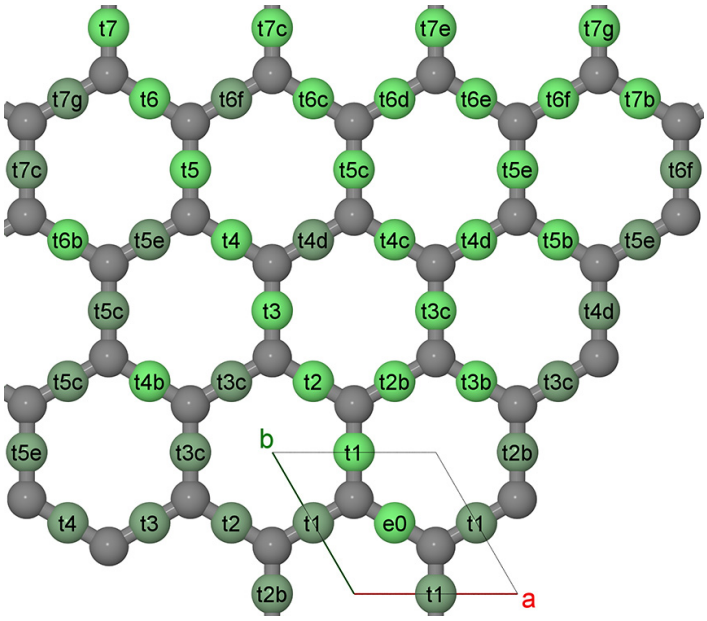

Figure 3: Symmetry unique TB elements of graphene σ-VB. See also Fig. 30.

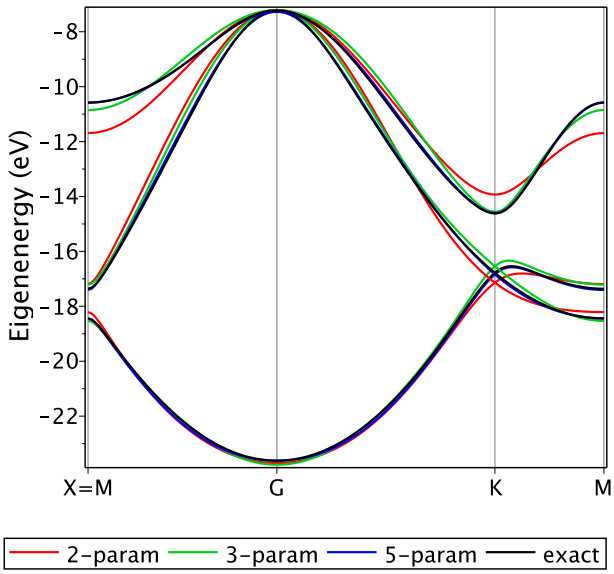

Figure 4: Energy bands of graphene σ-VB for a series of models of increasing accuracy.

The symmetry unique TB elements are shown in Fig. 3. There are 7 high-symmetry energy reference values at 3 k-points: Γ, K and M. At our best, we use 5-parameter model including 5 independent transfer integrals: t_1, t_2, t_{2b}, t_3 and t_{4d}. Other nonzero integrals include $t_{3b} = -t_3/2$, $t_{3c} = t_3/2$, $t_{4c} = t_3/2$, $t_4 = -t_3/3$, $t_5 = t_3/9$, $t_6 = -t_3/27$. This model fits high-symmetry points with 10 meV accuracy. With up to third-order terms, the Hamiltonian is given by

$$H_{11}(k_1,k_2,k_3) = \varepsilon_0 + 2t_2\left(\cos k_1 + \cos k_2\right) + 2t_{3c}\cos k_3,$$
$$H_{12} = t_1\left(1+\mathrm{e}^{\mathrm{i}k_2}\right) + t_{2b}\left(\mathrm{e}^{-\mathrm{i}k_1}+\mathrm{e}^{-\mathrm{i}k_3}\right) + t_3\left(\mathrm{e}^{-\mathrm{i}k_2}+\mathrm{e}^{\mathrm{i}2k_2}\right) + t_{3b}\left(\mathrm{e}^{\mathrm{i}k_1}+\mathrm{e}^{\mathrm{i}k_3}+\mathrm{e}^{\mathrm{i}(k_2-k_1)}+\mathrm{e}^{\mathrm{i}(k_2-k_3)}\right),$$
$$H_{22}(k_1,k_2,k_3) = H_{11}(k_2,k_3,k_1), \qquad H_{33}(k_1,k_2,k_3) = H_{11}(k_3,k_1,k_2),$$
$$H_{23}(k_1,k_2,k_3) = H_{12}(k_2,k_3,k_1), \qquad H_{31}(k_1,k_2,k_3) = H_{12}(k_3,k_1,k_2), \tag{3.1}$$

where $k_3 = -k_1 - k_2$. In high-symmetry points:

$$E_{1,2}(1/3,1/3) = \varepsilon_0 + t_1 - 2t_2 - 2t_{2b} - 2t_3 + 2t_{3b} - t_{3c}, \tag{3.2}$$
$$E_3(1/3,1/3) = \varepsilon_0 - 2t_1 - 2t_2 + 4t_{2b} + 4t_3 - 4t_{3b} - t_{3c}, \tag{3.3}$$
$$E_1(0,0) = \varepsilon_0 + 4t_1 + 4t_2 + 4t_{2b} + 4t_3 + 8t_{3b} + 2t_{3c}, \tag{3.4}$$
$$E_{2,3}(0,0) = \varepsilon_0 - 2t_1 + 4t_2 - 2t_{2b} - 2t_3 - 4t_{3b} + 2t_{3c}, \tag{3.5}$$
$$E_1(1/2,0) = \varepsilon_0 + 2t_1 - 2t_{2b} + 2t_3 - 4t_{3b} - 2t_{3c}, \tag{3.6}$$
$$E_2(1/2,0) = \varepsilon_0 - 4t_2 + 2t_{3c}, \tag{3.7}$$
$$E_3(1/2,0) = \varepsilon_0 - 2t_1 + 2t_{2b} - 2t_3 + 4t_{3b} - 2t_{3c}. \tag{3.8}$$

In particular, if we fit 5-parameter model to PBE/p2p calculations, we obtain (in eV):

$$\varepsilon_0 = -14.97,\ t_1 = -2.19,\ t_2 = 0.55,\ t_{2b} = -0.52,\ t_3 = -0.14,\ t_{4d} = 0.03,$$

giving band structure visually coinciding with the exact one. If we neglect 4-order integrals we come to reasonably accurate 3-parameter model: t_1, t_2, t_3 with $t_{2b} = -t_2$, $t_{3b} = -t_3/2$ and $t_{3c} = t_3/2$. The minimal is the 2-parameter model: t_1 and t_2 with $t_{2b} = -t_2$. Exact TB integrals fade with distance quickly:

$$\varepsilon_0 = -14.965,\ t_1 = -2.162,\ t_2 = 0.555,\ t_{2b} = -0.522,\ t_3 = -0.157,\ t_{3b} = 0.072,\ t_{3c} = -0.082,\ t_4 = 0.049,$$
$$t_{4c} = -0.049,\ t_{4d} = 0.024,\ t_{5c} = -0.020,\ t_{4b} = -0.010,\ t_6 = 0.008,\ t_{5b} = 0.005,\ t_{6b} = -0.002, \ldots$$

§4. Blue phosphorene valence band

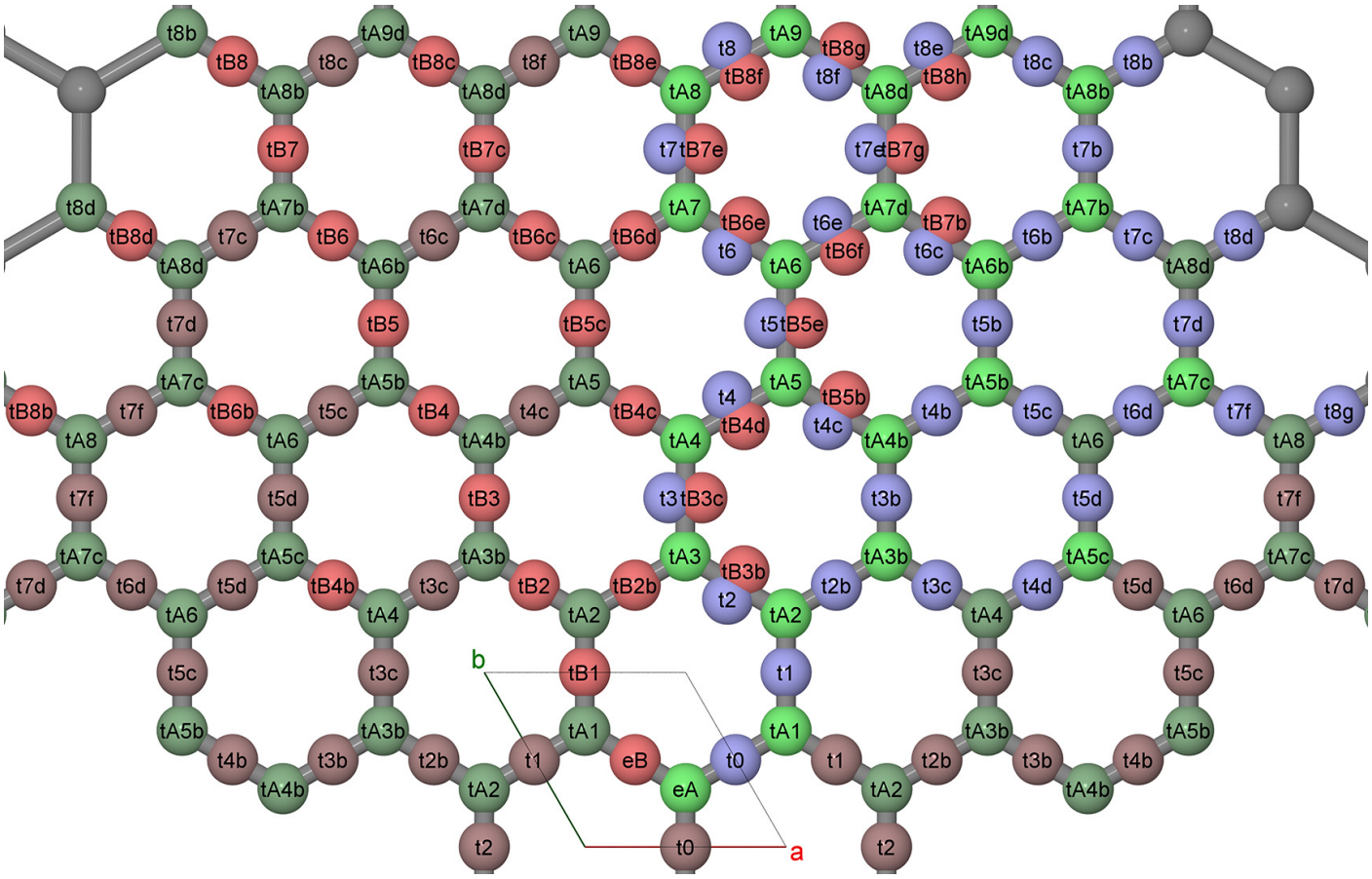

Figure 5: Symmetry unique TB elements of graphene atoms + bonds system. Here atom-atom elements are labeled with 'A' and colored in green, bond-bond elements are labeled with 'B' and colored in red, and atom-bond elements are colored in blue. Similar to other figures, the number in the labels shows chemical distance whereas the small letter after it indicates radial series. This set is complete to dimer separation 6.75 bond lengths and chemical distance 8. See also Fig. 31.

The valence band of 'blue' allotrope of phosphorene consists of σ-bonds and lone pairs, and thus its TB Hamiltonian has the same symmetry as TB Hamiltonian of atoms and bonds in graphene lattice, in the sense that the extra symmetry elements of p6/mmm layer group of graphene compared to p-3m1 group of phosphorene are factorized out as irrelevant internal symmetries. The symmetry unique TB elements are shown in Fig. 5.

There are 12 high-symmetry energy reference values at 3 k-points: Γ, K and M. However, those of them which intermix atoms and sites contain irreducible two-dimensional matrices.

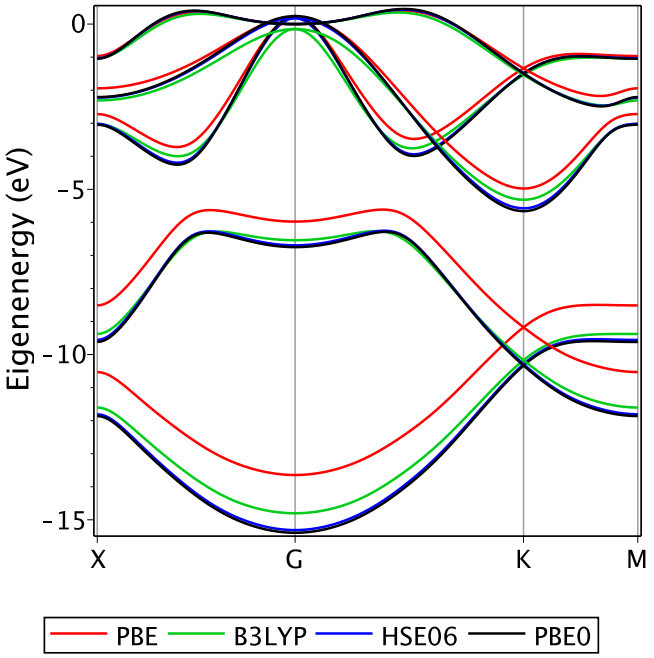

Figure 6: Energy bands of blue-P VB calculated with different density functionals in 'a3p' basis.

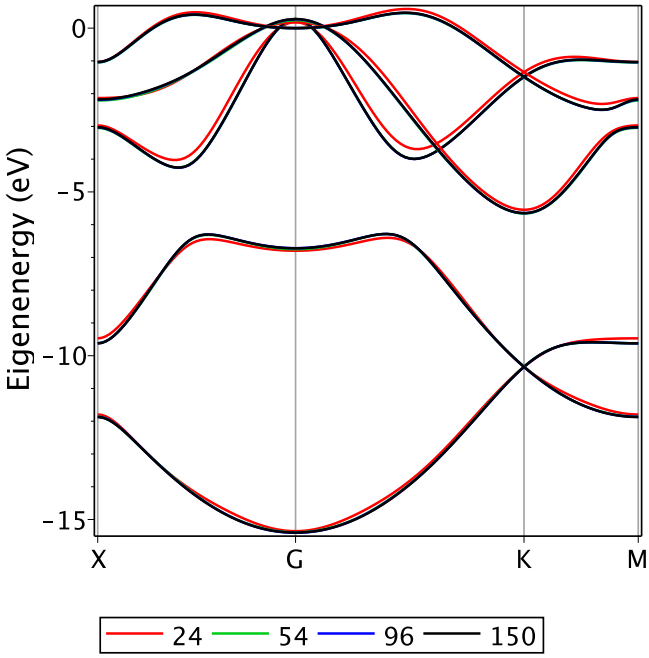

Figure 7: Energy bands of blue-P VB parameterized on high-symmetry H-passivated clusters of increasing size (number of P atoms).

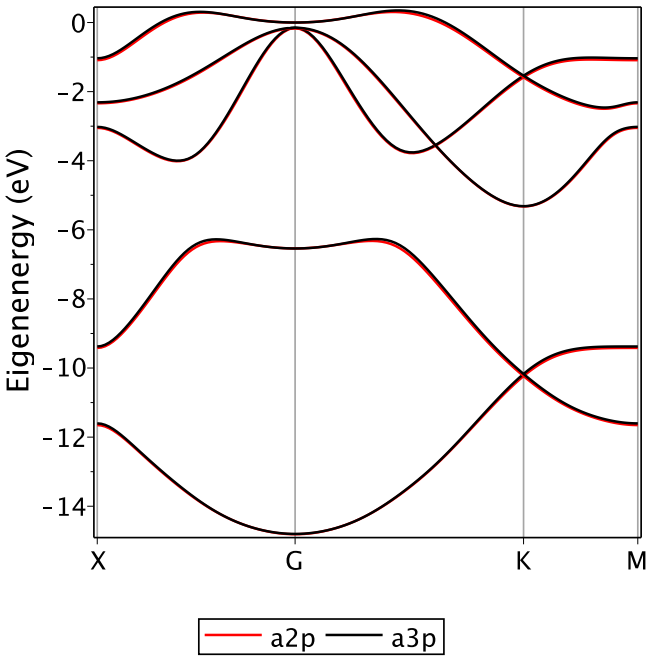

Figure 8: Dependence on basis set for B3LYP functional and cluster of 54 P atoms.

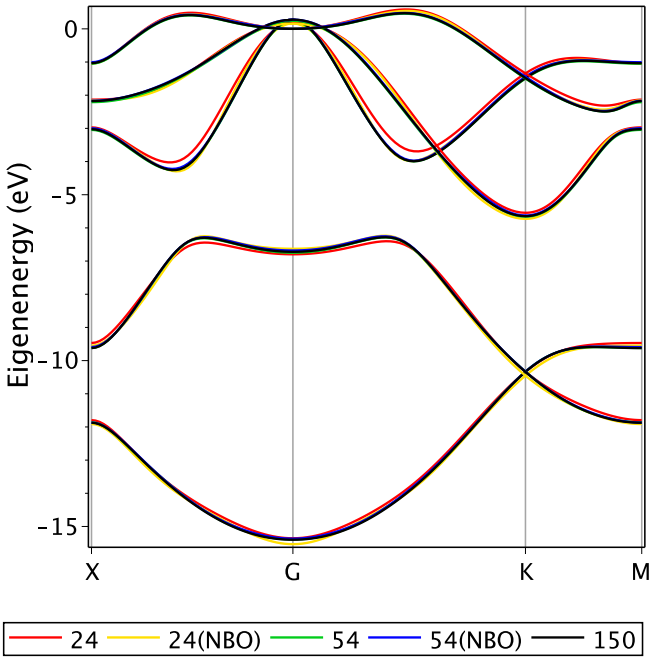

Figure 9: Dependence on coarse-graining method: NBO-projection vs. default 'inU' method.

§5. Honeycomb lattice with inversion

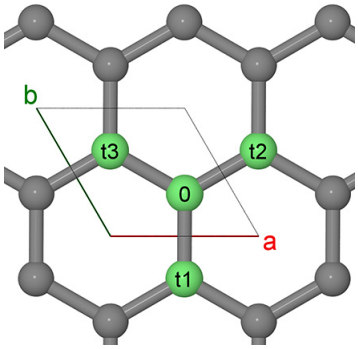

Figure 10: Symmetry unique TB elements of the simplest TB model on honeycomb lattice with inversion. See also Fig. 32.

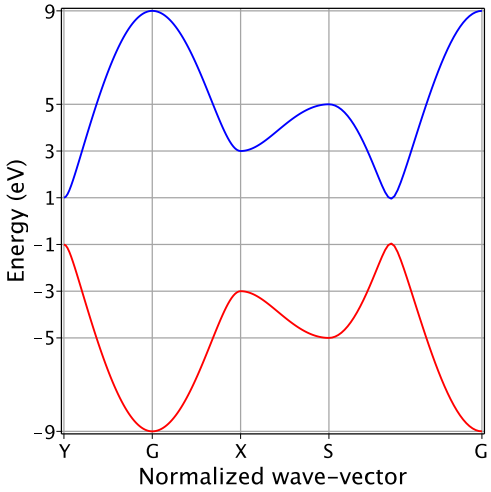

Figure 11: Energy bands for honeycomb lattice with $t_{1,2,3} = -4, -3, -2$.

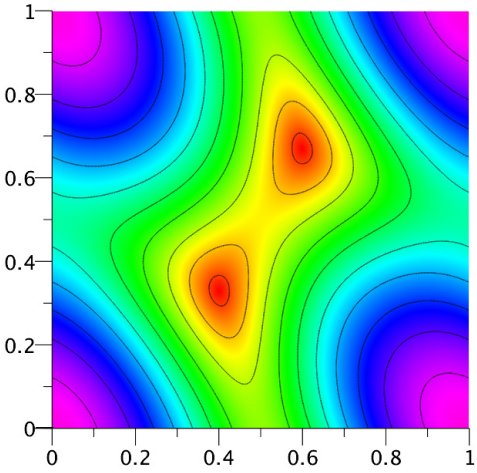

Figure 12: Lower energy band of the honeycomb lattice with $t_{1,2,3} = 1, 1.5, 1.7$.

The honeycomb lattice with inversion has two symmetry-equivalent sites and three different nearest neighbor couplings, Fig. 10. Let $\varepsilon_0 = 0$, then the elements of TB Hamiltonian are as follows

$$H_{11} = H_{22} = 0, \quad H_{12} = t_3 + t_2 \mathrm{e}^{\mathrm{i}k_1} + t_1 \mathrm{e}^{-\mathrm{i}k_2}. \tag{5.1}$$

There are two bands:

$$E_{1,2} = \mp\sqrt{t_1^2 + t_2^2 + t_3^2 + 2t_2t_3\cos k_1 + 2t_3t_1\cos k_2 + 2t_1t_2\cos k_3}, \quad k_3 = -k_1 - k_2. \tag{5.2}$$

The band structure is shown in Fig. 11, see also DOS on Fig. 23. The lower band, see Fig. 12, has at least four extrema per unit cell at points corresponding to $k_i = \pi n_i$, $n_i \in \mathbb{Z}$ and $E^2 = (\pm t_1 \pm t_2 \pm t_3)^2$ with 8 different sign combinations corresponding to 4 k-points per unit cell. If $|t_{1,2,3}|$ satisfy triangle inequality then and only then there is a fifth extremum, which is the maximum at $E = 0$ with k_i being angles or supplementary angles of the triangle with sides $|t_{1,2,3}|$, i.e. $2t_2t_3\cos k_1 = t_1^2 - t_2^2 - t_3^2$ and so fourth. In this case the two bands are interconnected at $E = 0$ via two Dirac cones per unit cell, otherwise the two bands are disconnected. Without the loss of generality, let $0 \leqslant t_1 \leqslant t_2 \leqslant t_3$, then the band edges are located at $E = \pm(t_1 + t_2 + t_3)$ and if $t_1 + t_2 < t_3$ then there is the band gap between $E = \pm(t_1 + t_2 - t_3)$, otherwise $t_1 + t_2 - t_3$ is the height of the Dirac cone relative to the nearest saddle point, which is the largest for the graphene lattice, i.e. when $t_1 = t_2 = t_3$.

For same-sign $t_{1,2,3}$ the band outer edges are at Γ-point, and mean effective masses are as follows:

$$\frac{1}{m_1} + \frac{1}{m_2} = \frac{a^2t_2t_3 + b^2t_3t_1 + |\boldsymbol{a} + \boldsymbol{b}|^2 t_1t_2}{t_1 + t_2 + t_3}, \quad \frac{1}{m_1 m_2} = \frac{|\boldsymbol{a} \times \boldsymbol{b}|^2 t_1t_2t_3}{t_1 + t_2 + t_3}. \tag{5.3}$$

Mean hopping amplitudes are given by

$$\eta_1^2 + \eta_2^2 = \frac{1}{2}\frac{a^2t_2^2t_3^2 + b^2t_3^2t_1^2 + |\boldsymbol{a} + \boldsymbol{b}|^2 t_1^2t_2^2}{t_1^2 + t_2^2 + t_3^2}, \quad \eta_1\eta_2 = \frac{1}{2}\frac{|\boldsymbol{a} \times \boldsymbol{b}| t_1t_2t_3}{\sqrt{t_1^2 + t_2^2 + t_3^2}}. \tag{5.4}$$

If site position is close to $(3/4, 1/4)$, the honeycomb lattice looks like a brickwork with bricks of the length close to $|\boldsymbol{a} - \boldsymbol{b}|/2$ and the height close to $|\boldsymbol{a} + \boldsymbol{b}|/2$, see Fig. 27.

§6. Triangular lattice with inversion

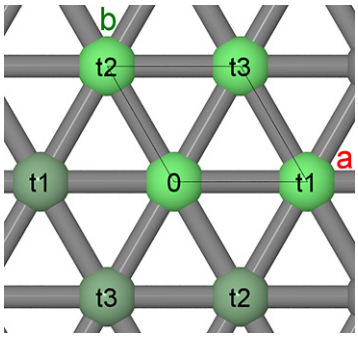

Figure 13: Symmetry unique TB elements of the simplest TB model on triangular lattice with inversion.

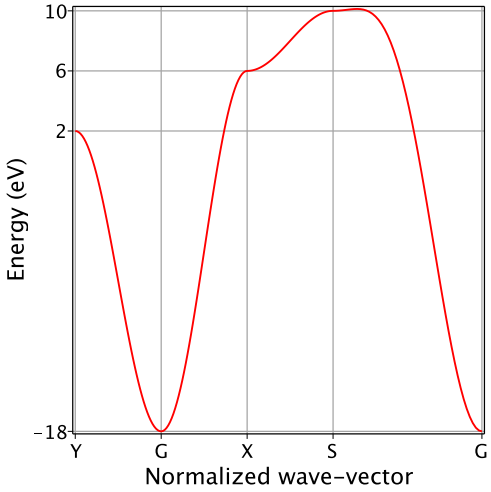

Figure 14: Energy bands for triangular lattice with $t_{1,2,3} = -4, -3, -2$.

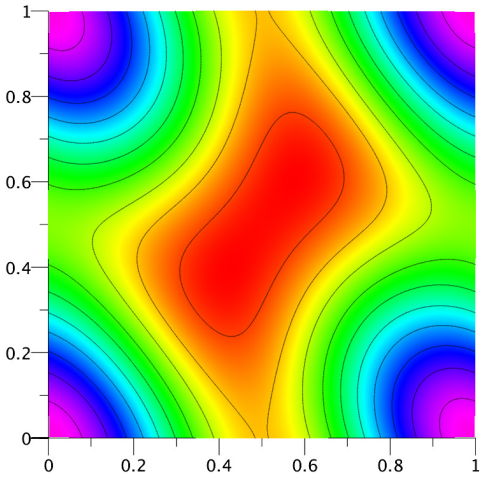

Figure 15: Lower energy band of the triangular lattice with $t_{1,2,3} = 1, 1.5, 1.7$.

The triangular lattice with inversion has one site per unit cell and three different nearest neighbor couplings, Fig. 13, which are assumed to be ordered as follows: $|t_1| > |t_2| > |t_3|$. Let $\varepsilon_0 = 0$, then the TB Hamiltonian is one-dimensional and its eigenenergy is given by

$$E = 2t_1 \cos k_1 + 2t_2 \cos k_2 + 2t_3 \cos k_3, \quad k_3 = -k_1 - k_2. \tag{6.1}$$

The band structure is shown in Fig. 14, see also DOS on Fig. 24. The lower band, see Fig. 15, has at least four extrema per unit cell at points corresponding to $k_i = \pi n_i$, $n_i \in \mathbb{Z}$ and $E = 2(\pm t_1 \pm t_2 \pm t_3)$ with even number of 'minus' signs corresponding to four k-points per unit cell. If $|t_{1,2,3}^{-1}|$ satisfy triangle inequality then and only then there is a fifth extremum with k_i satisfying the equations $t_1 \sin k_1 = t_2 \sin k_2 = t_3 \sin k_3$. In this case $k_i = \alpha_i + \pi \mathcal{I}\{t_1 t_2 t_3 / t_i > 0\}$, where $\alpha_{1,2,3}$ are angles of the triangle with sides $|t_{1,2,3}^{-1}|$. The energy of this extremum is given by $-t_1 t_2 / t_3 - t_2 t_3 / t_1 - t_3 t_1 / t_2$ and is close to $-2 \operatorname{sgn}(t_1 t_2 t_3)(|t_1| + |t_2| - |t_3|)$. The opposite extremun is at a high-symmetry point and has energy $2 \operatorname{sgn}(t_1 t_2 t_3)(|t_1| + |t_2| + |t_3|)$. Thus the band span is at least $4(|t_1| + |t_2|)$.

Mean effective masses at Γ-point are as follows:

$$\frac{1}{m_1} + \frac{1}{m_2} = 2a^2 t_1 + 2b^2 t_2 + 2|\boldsymbol{a} + \boldsymbol{b}|^2 t_3, \quad \frac{1}{m_1 m_2} = 4|\boldsymbol{a} \times \boldsymbol{b}|^2 (t_1 t_2 + t_2 t_3 + t_3 t_1). \tag{6.2}$$

Mean hopping amplitudes are given by

$$\eta_1^2 + \eta_2^2 = a^2 t_1^2 + b^2 t_2^2 + |\boldsymbol{a} + \boldsymbol{b}|^2 t_3^2, \quad \eta_1 \eta_2 = |\boldsymbol{a} \times \boldsymbol{b}|^2 \left(t_1^2 t_2^2 + t_2^2 t_3^2 + t_3^2 t_1^2\right). \tag{6.3}$$

§7. Diamond σ-valence band

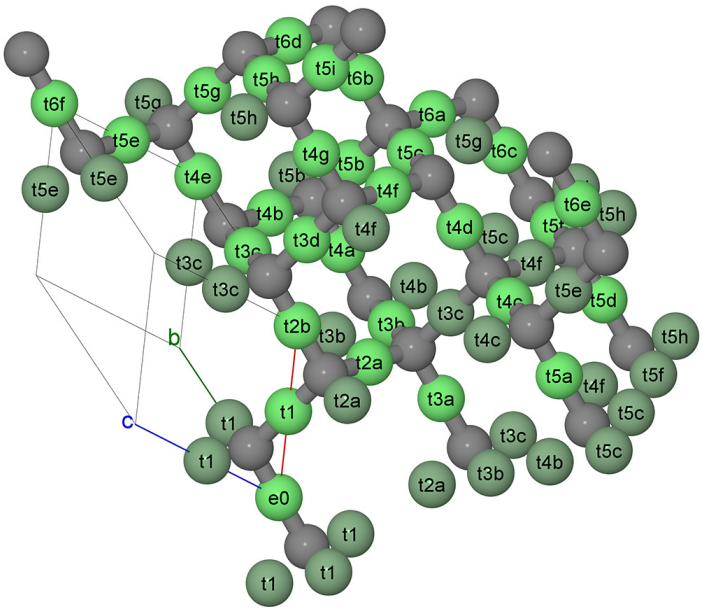

Figure 16: Symmetry unique TB elements of diamond σ-VB. See also Fig. 33.

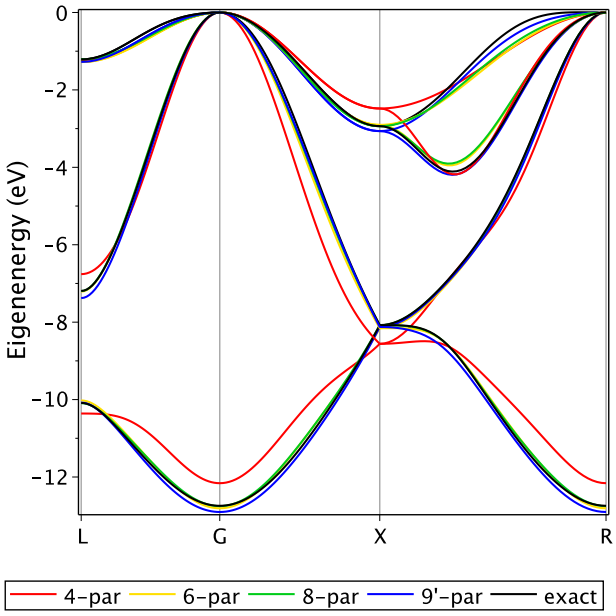

Figure 17: Energy bands of Si-diamond σ-VB: comparison of three models parameterized by high-symmetry points (4-,6-,8-par) and a 9-parameter model where all TB elements higher than 10 meV are copied from the exact TB Hamiltonian (9'-par).

The symmetry unique TB elements are shown in Fig. 16. There are 9 high-symmetry energy reference values at 4 k-points: Γ, X, W and L. The minimal model free of accidental degeneracy includes 4 parameters: e_0, t_1, t_{2b}, t_{3d}, and this model produces qualitatively correct bands as shown in Fig. 17. Addition of more parameters fitted at high-symmetry points improves the accuracy near those points, but no systematic improvement of accuracy of X-R k-path is observed, see Fig. 17.

The effective mass at the nondegenerate Γ-point state is given by

$$\frac{1}{ma^2} = -\frac{t_1 + 4t_{2b} + 9t_{3d}}{4}. \tag{7.1}$$

At the triply degenerate Γ-point state the three-dimensional Hamiltonian is given by the following symmetry-unique elememts:

$$\frac{H_{11}}{a^2} = \frac{t_1 - 4t_{2b} + 9t_{3d}}{4} k_1^2 - t_{2b}\left(k_2^2 + k_3^2\right), \quad \frac{H_{12}}{a^2} = \frac{t_1 - 4t_{2b} + 9t_{3d}}{4} k_1 k_2, \tag{7.2}$$

where $\boldsymbol{k}$ is Cartesian wave vector.

§8. K4 lattice or Laves graph

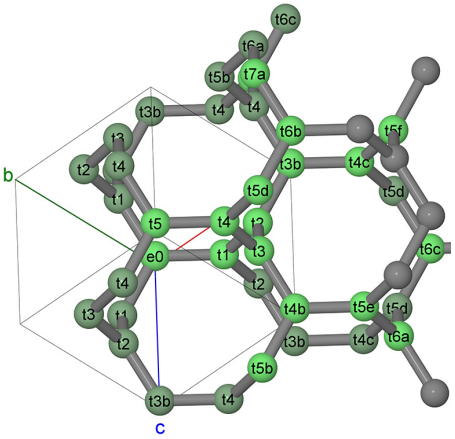

Figure 18: Symmetry unique TB elements of K4 lattice.

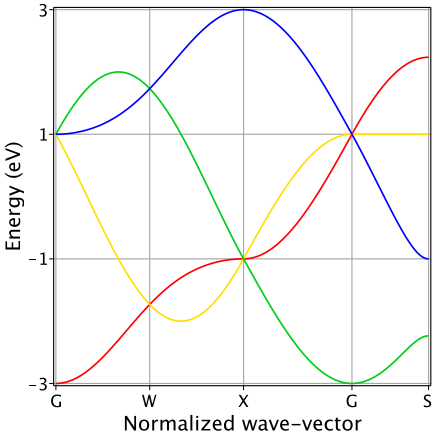

Figure 19: Energy bands of K4 lattice with $t_1 = -1$.

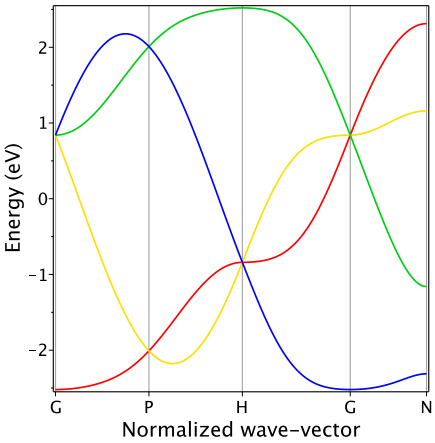

Figure 20: Energy bands of K4 lattice with $t_1 = -1, t_2 = 0, t_3 = 2/25$.

The K4 lattice has four symmetry-equivalent sites per primitive cell. In the nearest neighbor model with $\varepsilon_0 = 0$ and $t_1 = t$, the Hamiltonian reads

$$H_{ii} = 0,\ i = \overline{1,4}, \quad H_{1i} = t,\ i = \overline{2,4}, \quad H_{42} = te^{-ik_1},\ H_{23} = te^{-ik_2},\ H_{34} = te^{-ik_3}. \tag{8.1}$$

The eigenvalues satisfy the equation

$$(E-3t)(E+t)^3 + (E+t)t^3\sum_{i=1}^{4}\kappa_i^2 = t^4\prod_{i=1}^{4}\kappa_i, \quad \kappa_i = 2\sin\frac{k_i}{2}, \quad k_4 = -k_1-k_2-k_3. \tag{8.2}$$

At Γ-point there is one simple eigenvalue and three degenerates solutions including Dirac cone and non-quadratic branch:

$$E_0 = 3t,\ E_\pm = -t \pm \frac{tk}{2},\ E_1 = -t + \frac{tk_1k_2k_3k_4}{k^2}, \quad k^2 = \sum_{i=1}^{4}k_i^2 \equiv \sum_{i\leqslant j=1}^{3}k_ik_j. \tag{8.3}$$

Note that k^2 is positive-definite quadratic form. See the band structure in Fig. 19.

The minimal model free of accidental degeneracy and electron-hole symmetry includes 4 parameters: e_0, t_1, t_2, t_3. The effective mass at the nondegenerate Γ- and H-point states are given by

$$\frac{1}{ma^2} = -\frac{t_1+6t_2+10t_3}{8} \text{ and } \frac{1}{ma^2} = \frac{t_1-6t_2+10t_3}{8} \text{ respectively.} \tag{8.4}$$

§9. Orthorhombic lattice with K4 topology

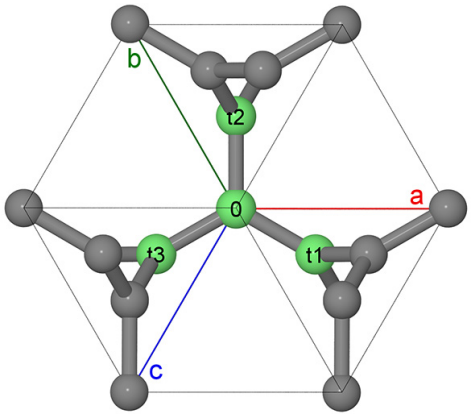

Figure 21: Symmetry unique TB elements of the simplest TB model on K4o lattice. Note that primitive cell is shown here, whereas a, b, c parameters in the text corresponds to the Bravais cell.

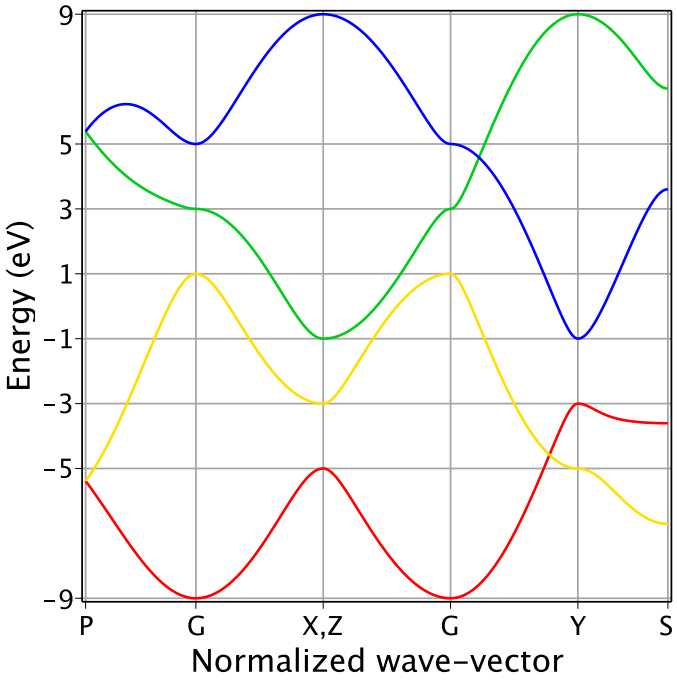

Figure 22: Energy bands for K4o lattice with $t_{1,2,3} = -4, -3, -2$.

The symmetry of the orthorhombic lattice with K4 topology (K4o lattice) is reduced to $I2_12_12_1$ compared to $I4_132$ for perfect K4. It has three different nearest neighbor couplings, Fig. 21. The triple degeneracy of the fully symmetric K4 model is completely removed in a generic K4o lattice, Fig. 22. Energy levels at Γ- and H-points (H=X=Y=Z) are equal to $\pm t_1 \pm t_2 \pm t_3$ with even and odd number of 'minus' signs, respectively. One of the two band extrema (minimum or maximum) is at the Γ-point and the opposite extremum is at the H-point (H=X=Y=Z). Consequently, the entire band spans from $-|t_1| - |t_2| - |t_3|$ to $|t_1| + |t_2| + |t_3|$. There are two Dirac cones at P-point with $E = \pm\sqrt{t_1^2 + t_2^2 + t_3^2}$. The DOS has four bands: two near band extrema and another two in level crowding regions corresponding to triply degenerate points of the ideal K4 lattice, see Figs. 25 and 26.

The effective masses at the band extrema are

$$\frac{1}{m_1} = \pm\frac{a^2}{4}\frac{|t_1 t_3|}{|t_1| + |t_3|}, \quad \frac{1}{m_2} = \pm\frac{b^2}{4}\frac{|t_2 t_1|}{|t_2| + |t_1|}, \quad \frac{1}{m_3} = \pm\frac{c^2}{4}\frac{|t_3 t_2|}{|t_3| + |t_2|}. \tag{9.1}$$

The hopping amplitudes are

$$\eta_1^2 = \frac{a^2}{8}\frac{t_1^2 t_3^2}{t_1^2 + t_3^2}, \quad \eta_2^2 = \frac{b^2}{8}\frac{t_2^2 t_1^2}{t_2^2 + t_1^2}, \quad \eta_3^2 = \frac{c^2}{8}\frac{t_3^2 t_2^2}{t_3^2 + t_2^2}. \tag{9.2}$$

If site position in the Bravais cell is close to $(1/4, 0, 0)$, the K4o lattice looks like a wiremesh in ab-plane with links of the length close to $\sqrt{a^2 + b^2}/2$ separated vertically by $c/4$ on average, see Fig. 28.

Appendix

§A. Nonorthogonal basis set

A tight-binding Hamiltonian with an orthogonal basis needs substantial re-parameterization upon changing the geometry as compared to the basis of atomic-like orbitals (see [1] and recent discussions in [2]). This concerns in particular defects and boundaries. However, modern semiempirical programs such as MOPAC assume orthogonal basis and give accurate geometries for the wide range of molecules and crystals even being parameterized universally.

The most commonly used is the symmetric (Lowdin) orthogonalization: if S is the overlap matrix then $H' = S^{-1/2}HS^{-1/2}$ is the orthogonalized Hamiltonian. To understand the influence of nonorthogonal basis set, let consider a semi-infinite linear chain with the following nonzero matrix elements:

$$H_{nn} = \varepsilon,\ H_{n,n+1} = H_{n+1,n} = -t, \quad S_{nn} = 1,\ S_{n,n+1} = S_{n+1,n} = s, \quad n \in \mathbb{N}.$$

Then

$$H'_{nm} = \varepsilon\delta_{nm} + \frac{t+s\varepsilon}{s}\left[\frac{1+q^2}{1-q^2}\left(q^{|n-m|} - q^{n+m}\right) - \delta_{nm}\right], \qquad q = -\frac{2s}{1+\sqrt{1-4s^2}}.$$

The intersite matrix elements of this Hamiltonian decrease with distance exponentially as $q^{|n-m|}$. The diagonal and nearest neighbor elements are renormalized as follows:

$$H'_{nn} = \varepsilon + t'(2s + q^{2n-1}), \quad H'_{n,n+1} = -t'(1-q^{2n}), \qquad t' = (t+s\varepsilon)\left|\frac{q}{s}\right|\frac{1+q^2}{1-q^2}.$$

In particular, the edge site ($n = 1$) has additional shift relative to sites in the bulk.

§B. Participation ratio

For a given normalized wave-function ψ the participation ratio, defined by

$$p = \left(\sum_n |\psi_n|^4\right)^{-1},$$

is the measure of the localization length of ψ. For example, if $\psi_n = 1/\sqrt{L}$, $n = \overline{1,L}$, then $p = L$. If

$$\psi_n = \sqrt{\frac{1-q^2}{1+q^2}}q^{|n|},\ n \in \mathbb{Z},\ \text{then } p = \frac{\left(1+q^2\right)^4}{1-q^8} \approx 2R \ \text{ for } R = \frac{1}{\ln|q^{-1}|} \gg 1.$$

§C. Additional figures and tables

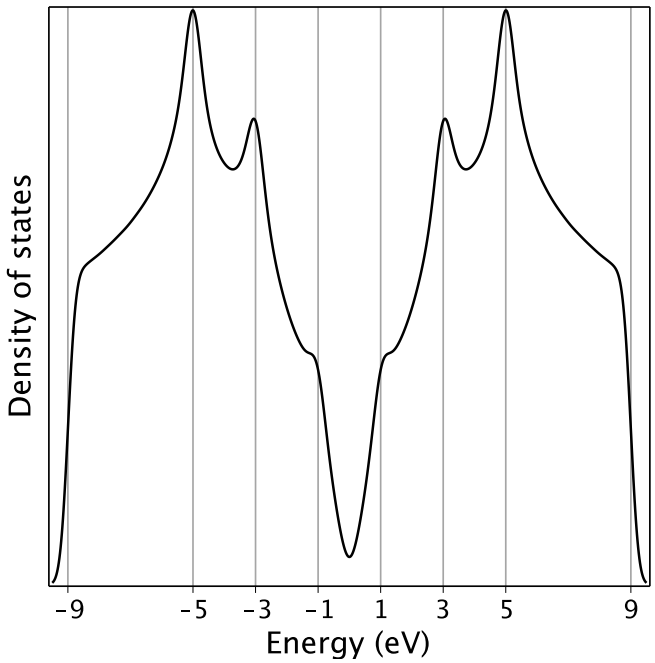

Figure 23: DOS for honeycomb lattice with $t_{1,2,3} = -4, -3, -2$.

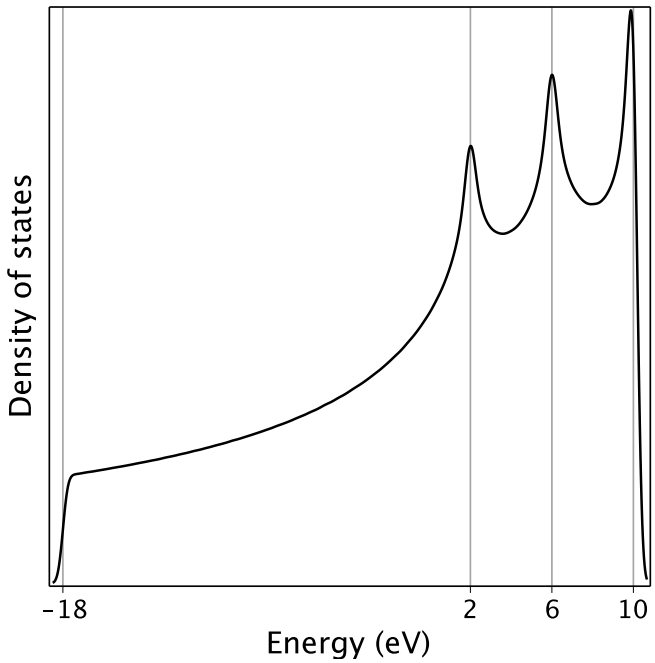

Figure 24: DOS for triangular lattice with $t_{1,2,3} = -4, -3, -2$.

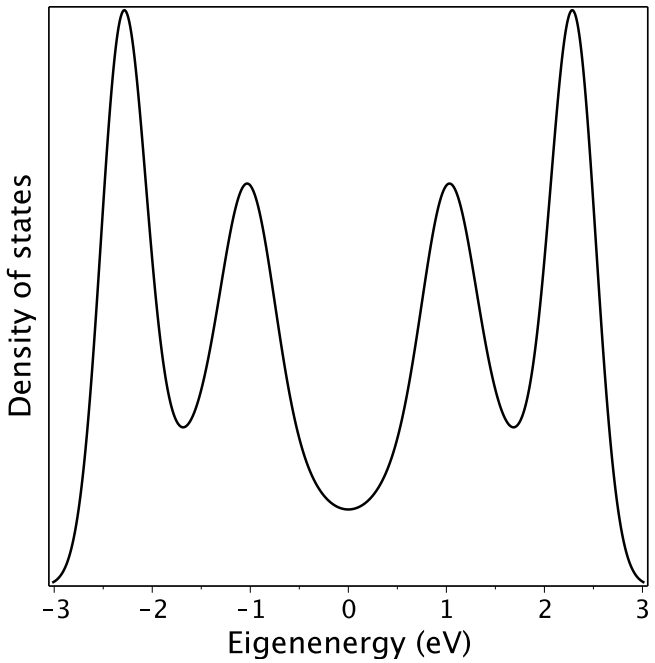

Figure 25: DOS for K4 lattice with $t_1 = -1, t_2 = 0, t_3 = 2/25$.

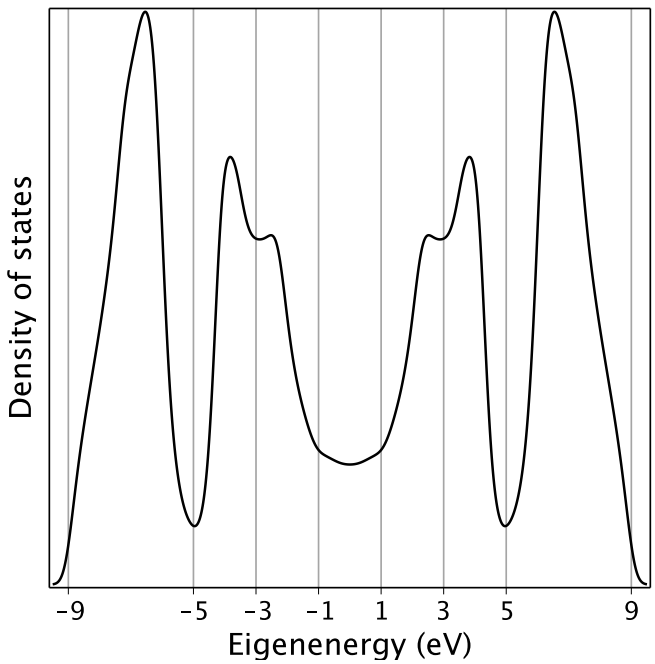

Figure 26: DOS for K4o lattice with $t_{1,2,3} = -4, -3, -2$.

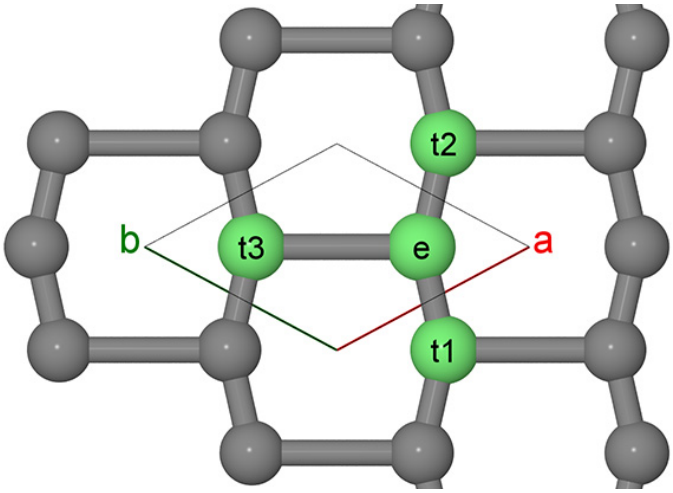

Figure 27: Honeycomb lattice in brickwork settings.

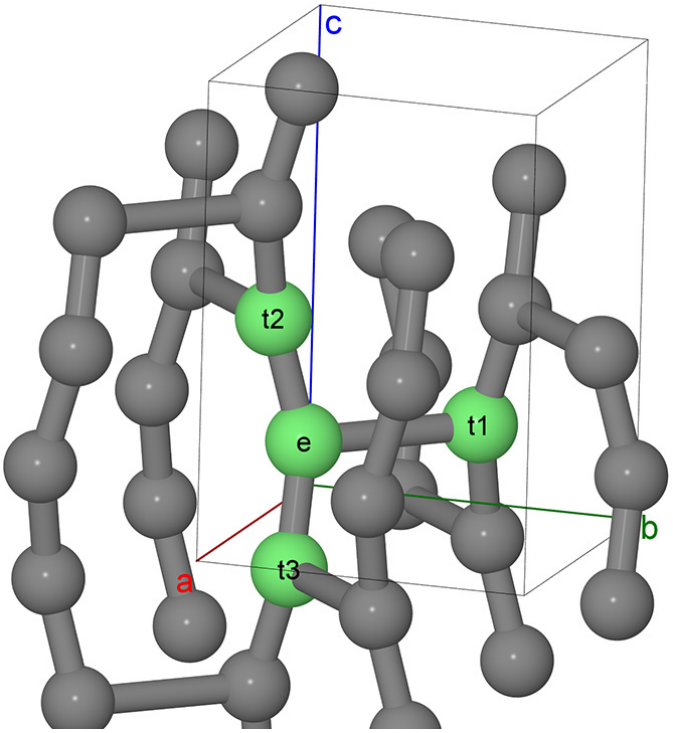

Figure 28: K4o lattice in wiremesh settings.

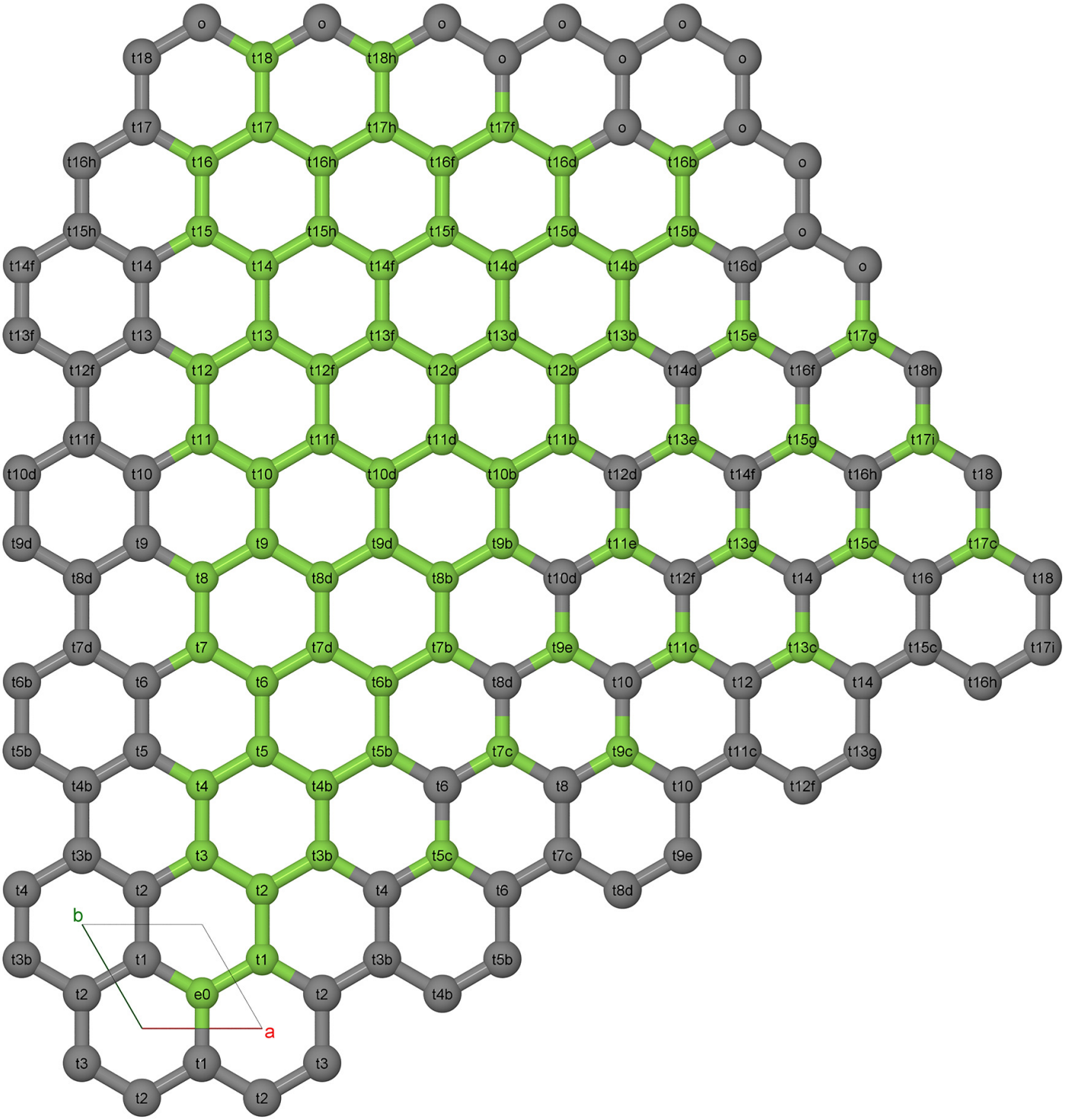

Figure 29: Symmetry unique TB elements of graphene π-system.

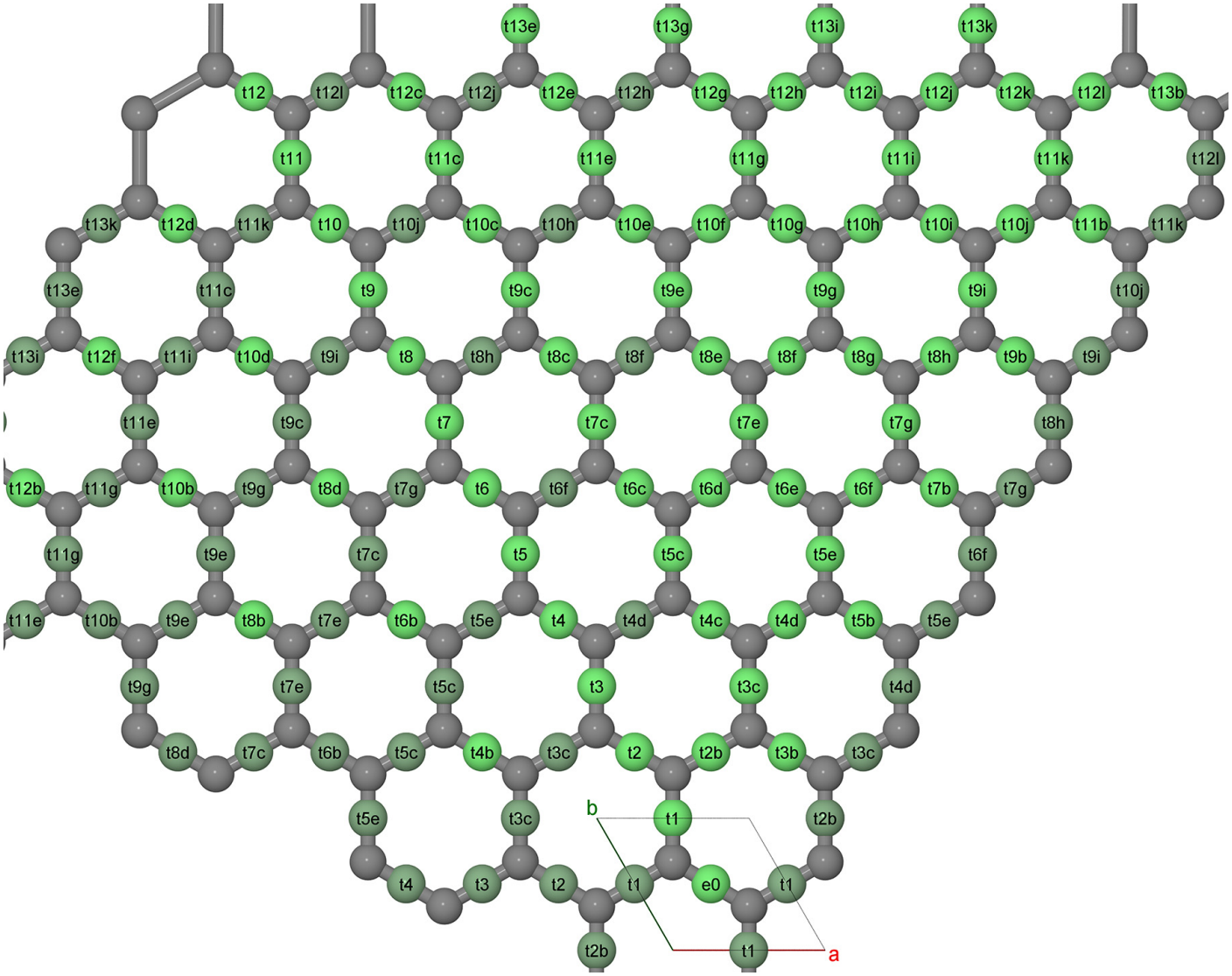

Figure 30: Symmetry unique TB elements of graphene σ-system.

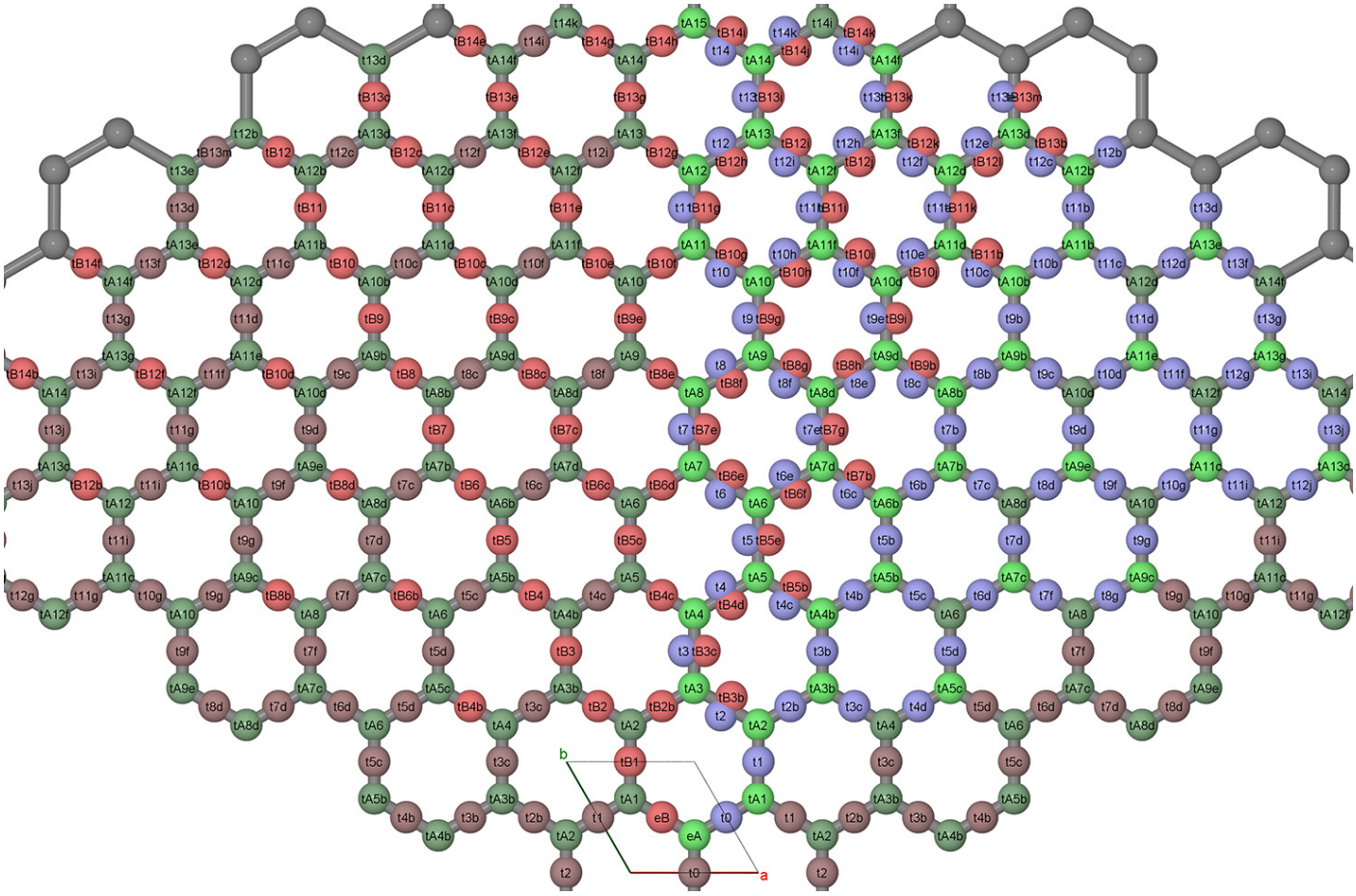

Figure 31: Symmetry unique TB elements of graphene atom and bonds.

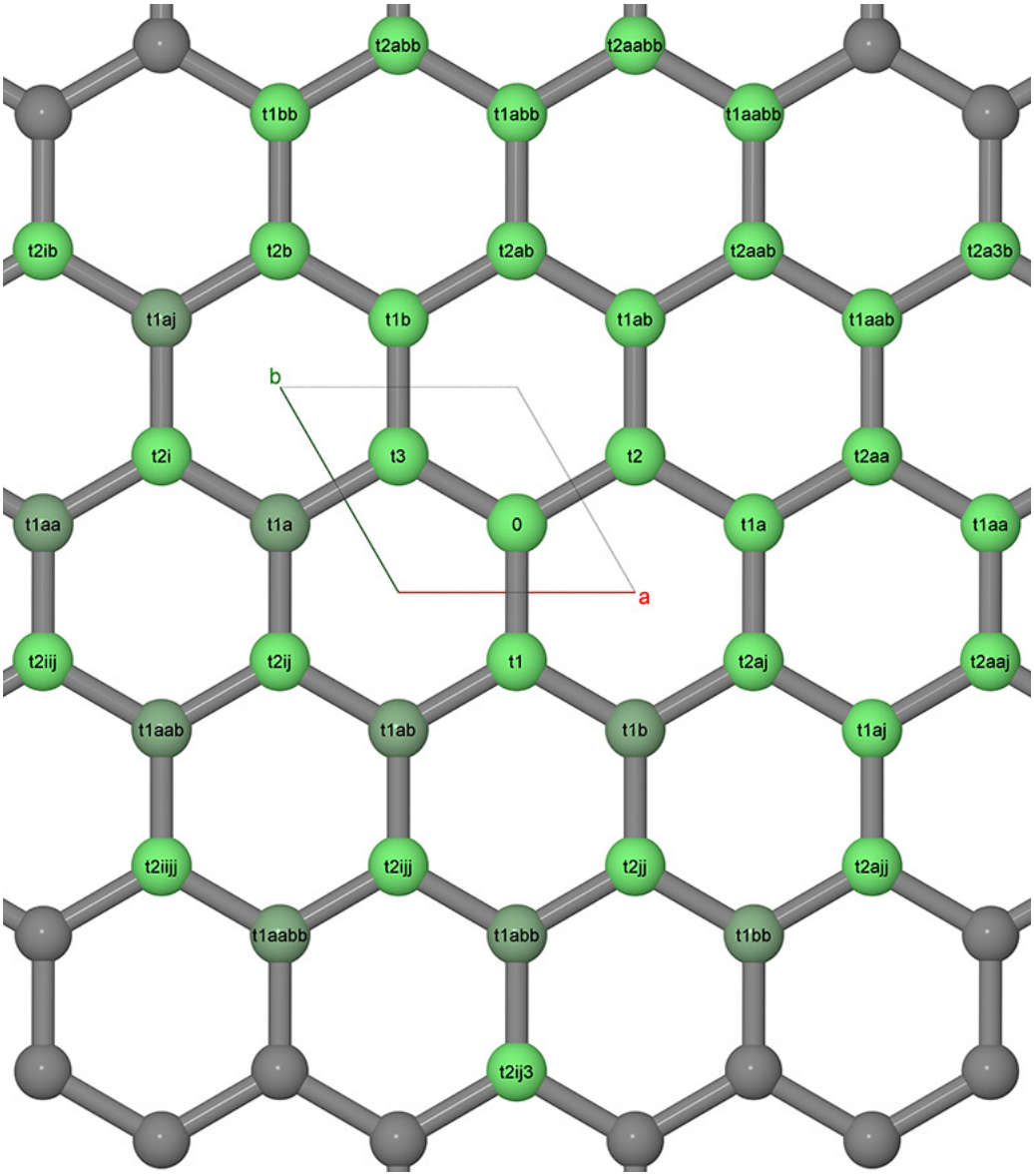

Figure 32: Symmetry unique TB elements of the simplest TB model on honeycomb lattice with inversion.

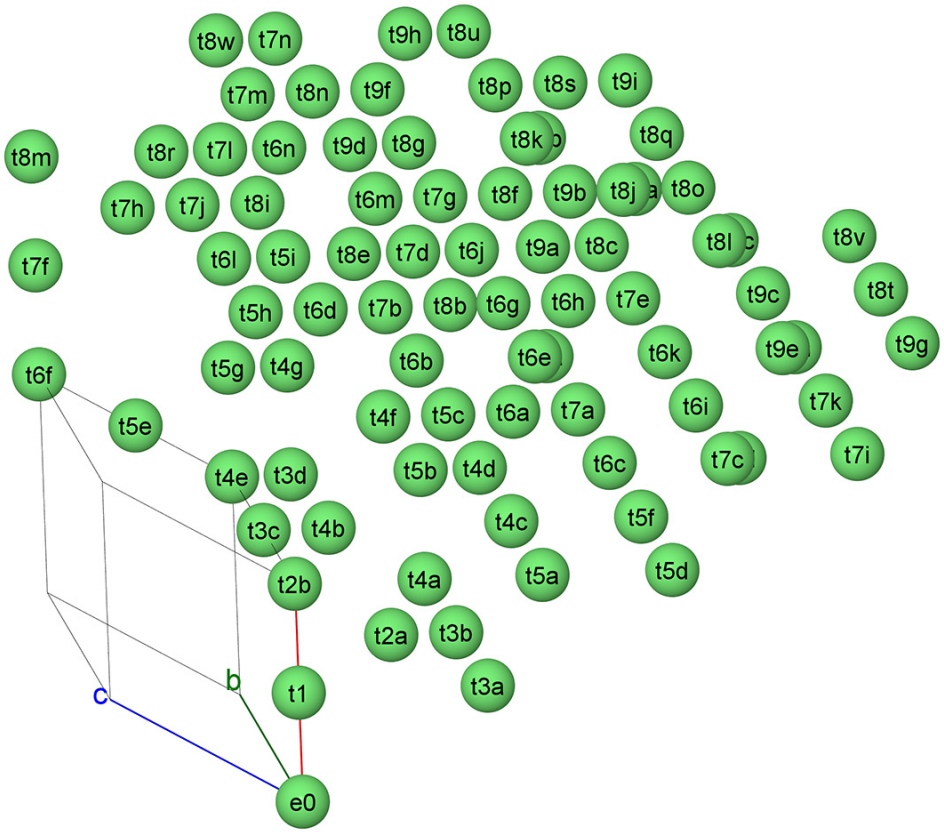

Figure 33: Symmetry unique TB elements of diamond σ-VB.

References

[1] A Zhugayevych, Fundamental models of quantum chemistry

[2] D Kienle, J I Cerda, A W Ghosh, Extended Huckel theory for band structure, chemistry, and transport. I. Carbon nanotubes, J Appl Phys 100, 043714 (2006)